MICROSTRUCTURAL AND ELASTIC PROPERTIES OF SHORT FIBER REINFORCED COMPOSITES

V. Müller*[1], T. Böhlke[1]

[1] *Institute of Engineering Mechanics, Chair for Continuum Mechanics, Karlsruhe Institute of Technology (KIT)*

* *Corresponding Author: viktor.mueller@kit.edu*

Keywords: two-scale modeling, homogenization, self-consistence method, fiber-reinforced composite, fiber orientation distribution, maximum entropy method

Abstract

The main contribution of this work is the prediction of the linear elastic properties of short fiber-reinforced composites (SFRCs) and the estimation of the fiber orientation distribution function (FODF) based only on fiber orientation tensors of second order. A SFRC consisting of polypropylene with 30*wt% of short glass fibers is considered exemplary. In the first part, two micromechanically based mean field methods are applied to approximate the linear elastic properties of the composite. Both presented methods, the self-consistence method and a two-step bounding approach, are able to consider segmented microstructure date from, e.g., micro computer tomography measurements. In the second part, it is shown, how the FODF can be estimated without closure approximations using the maximum entropy method (MEM).*

1. Homogenization of short fiber-reinforced composites

1.1. Introduction

Short fiber-reinforced composites (SFRCs) are steadily used for more and more applications. Due to the fact, that SFRCs show heterogeneities on different length scales concerning microstructural properties like fiber volume fraction and fiber orientation distribution, a robust dimensioning of light-weight structures with reinforced materials is still a challenging task.

In this paper, different micromechanically based mean field approaches are utilized in order to model a composite material consisting of 30wt.-% of glass fibers reinforcing a polypropylene matrix (PPGF30). The models operate on microstructure data from micro-computer tomography (μCT) measurements, which are used to extract the aspect ratio and the orientation of the fibers [7]. The effective linear elastic properties are determined by the self-consistence method and a two-step bounding approach. The numerical results are compared with experimental results out of tensile test.

1.2. Self-Consistence Homogenization

The microstructure of the SFRC can be characterized by a distinct matrix and N fibers with the stiffness tensors $\mathbb{C}_\mathsf{M}$ and $\mathbb{C}_\alpha$, respectively. Each fiber, constituted by the fiber axis $\boldsymbol{n}_\alpha$ and the fiber aspect ratio a_α, is separately used in the SC scheme.

Following [11], the effective elastic stiffness $\bar{\mathbb{C}}$ can by calculated exactly for the given composite by

$$\bar{\mathbb{C}} = \mathbb{C}_\mathsf{M} + \sum_{\alpha=1}^{N} c_\alpha \left(\mathbb{C}_\alpha - \mathbb{C}_\mathsf{M}\right) \mathbb{A}_\alpha. \tag{1}$$

In the last equation, c_α is the volume fraction of each fiber. The fourth-order tensor $\mathbb{A}_\alpha$ is called strain localization tensor. For ellipsoidal inclusions, $\mathbb{A}_\alpha$ is available explicitly. With the approximation of the cylindrical fibers through ellipsoids with equal volume and length like the cylinder, and the assumption, that each fiber is embedded in an infinite homogeneous matrix consisting of the effective material $\mathbb{C}^\mathsf{SC}$, the strain localization tensor $\mathbb{A}_\alpha$ depends on the effective material $\mathbb{C}^\mathsf{SC}$, the fiber material $\mathbb{C}_\alpha$, the orientation of the fiber axis $\boldsymbol{n}_\alpha$ and the fiber aspect ratio a_α. Considering these assumptions in equation (1), and replacing the exact $\bar{\mathbb{C}}$ with the approximating $\mathbb{C}^\mathsf{SC}$ gives the implicit equation for the effective linear elastic stiffness:

$$\mathbb{C}^\mathsf{SC} = \mathbb{C}_\mathsf{M} + \sum_{\alpha=1}^{N} c_\alpha \left(\mathbb{C}_\alpha - \mathbb{C}_\mathsf{M}\right) \left(\mathbb{I}^\mathsf{s} + \mathbb{P}_0^\mathsf{SC} \left(\mathbb{C}_\alpha - \mathbb{C}^\mathsf{SC}\right)\right)^{-1}. \tag{2}$$

$\mathbb{P}_0^\mathsf{SC}$ is called polarization tensor. This quantity depends on the geometry of the ellipsoidal representation of the fiber and the effective material $\mathbb{C}^\mathsf{SC}$ (see [11]). This equation is solved numerically using a damped Newton-Raphson method.

1.3. A Two-Step Bounding Method

In the first step the microstructure is decomposed into as many domains as there are different inclusions or fibers, respectively. The volume fraction of the matrix attributed to each fiber corresponds to the volume fraction of the total matrix fraction $c_\mathsf{M} = 1 - c_\mathsf{F}$. Each pair of a fiber and the surrounding matrix material is homogenized by applying the unidirectional (UD) special case of the second-order Hashin-Shtrikman (HS) bounds [8]:

$$\mathbb{C}_\alpha^{\mathsf{UD}-} = \mathbb{C}_\mathsf{M} + c_\mathsf{F} \left(\mathbb{C}_\alpha - \mathbb{C}_\mathsf{M}\right) \mathbb{A}_\alpha^-, \qquad \mathbb{C}_\alpha^{\mathsf{UD}+} = \mathbb{C}_\mathsf{I} + (1 - c_\mathsf{F}) \left(\mathbb{C}_\mathsf{M} - \mathbb{C}_\alpha\right) \mathbb{A}_\alpha^+. \tag{3}$$

$\mathbb{A}_\alpha^+$ and $\mathbb{A}_\alpha^-$ are the strain localization tensors:

$$\mathbb{A}_\alpha^- = \left(\mathbb{I}^\mathsf{s} + (1 - c_\mathsf{F})\, \mathbb{P}^\mathsf{UD} \left(\mathbb{C}_\alpha - \mathbb{C}_\mathsf{M}\right)\right)^{-1}, \qquad \mathbb{A}_\alpha^+ = \left(\mathbb{I}^\mathsf{s} + c_\mathsf{F}\, \mathbb{P}^\mathsf{UD} \left(\mathbb{C}_\mathsf{M} - \mathbb{C}_\alpha\right)\right)^{-1}. \tag{4}$$

The polarization tensor $\mathbb{P}^\mathsf{UD}$ is explicitly known for the UD case [8]. The elastic behavior of the domains, denoted by $\mathbb{C}_\alpha^\mathsf{UD}$ is transversely isotropic. The homogenization of the elastic behavior of the aggregate of domains is done by applying the HS-scheme for granular microstructures [8]. Only corresponding predictions are combined: the lower bound for the domains is homogenized with the lower HS bound for the aggregate, whereas the upper bound is homogenized with the

Table 1. Elastic properties for glass from [9] and measured linear elastic properties for PP and PPGF30.

	E [GPa]	ν
Glass	73.0	0.22
PP	1.665	0.364
PPGF30 (0°)	4.482	0.271
PPGF30 (90°)	3.452	0.217
PPGF30 (45°)	3.540	0.304

upper HS bound. The stiffness tensors are denoted by $\mathbb{C}^{\mathsf{HS}++}$ and $\mathbb{C}^{\mathsf{HS}--}$, respectively:

$$\mathbb{C}^{\mathsf{HS}\pm} = \sum_{\alpha=1}^{N} \frac{c_\alpha}{c_\mathsf{F}} \mathbb{C}_\alpha^{\mathsf{UD}\pm} \mathbb{A}_\alpha^{\pm} = \sum_{\alpha=1}^{N} \frac{c_\alpha}{c_\mathsf{F}} \mathbb{C}_\alpha^{\mathsf{UD}\pm} \mathbb{M}_\alpha^{\pm} \langle \mathbb{M}^{\pm} \rangle^{-1} , \tag{5}$$

with

$$\mathbb{M}_\alpha^{\pm} = \left(\mathbb{I}^{\mathsf{s}} + \mathbb{P}_0 (\mathbb{C}_\alpha^{\mathsf{UD}\pm} - \mathbb{C}_0^{\pm}) \right)^{-1} , \qquad \langle \mathbb{M}^{\pm} \rangle = \sum_{\beta=1}^{N} \frac{c_\beta}{c_\mathsf{F}} \left(\mathbb{I}^{\mathsf{s}} + \mathbb{P}_0 (\mathbb{C}_\beta^{\mathsf{UD}\pm} - \mathbb{C}_0^{\pm}) \right)^{-1} . \tag{6}$$

Now, $\mathbb{P}_0$ is the polarization tensor for a spherical inclusion, which is embedded in a matrix with the material $\mathbb{C}_0^{\pm}$. In case of the upper HS bound, for this material the maximum isotropic part of all $\mathbb{C}_\alpha^{\mathsf{UD}+}$ is taken. Otherwise, for the lower HS bound of the aggregate, $\mathbb{C}_0^{\pm}$ is equal to the minimum isotropic part of all $\mathbb{C}_\alpha^{\mathsf{UD}-}$.

1.4. Measured Microstructure

Usually, the manufacturing of injection molded thin plates, made of SFRC, results in a cross section, the microstructure of which shows three characteristic sections: Near the walls of the plate, the fibers are mainly oriented in flow direction of the material, but in the core section, the orientation of the fibers is predominantly perpendicular to the flow direction. This observation is also apparent from the reconstruction of the μCT data in Fig. 1(a). In order to get this information, a cylindrical specimen with a diameter $D = 4$mm has been measured by μCT with a resolution of 1.8μm. Then, from this 3D voxel data the position, the axis orientation, the length and the diameter of a statistically representative set of the fibers have been determined.

1.5. Results and comparison

In Tab. 1 the elastic constants of the glass fibers and the polymeric matrix, which have been used within the homogenization procedure, and the measured properties of the composite in three directions are given. The measured data have been obtain from tensile test in the filling direction during injection molding (0°), the transverse direction (90°), and a third direction (45°). In order to compare the elastic properties of the composite for each homogenized elastic stiffness, the direction-dependent Youngs modulus $E(\boldsymbol{d})$ has been calculated and evaluated in the corresponding directions [3]:

$$\frac{1}{E(\boldsymbol{d})} = \boldsymbol{d} \otimes \boldsymbol{d} \cdot \mathbb{S} [\boldsymbol{d} \otimes \boldsymbol{d}] , \tag{7}$$

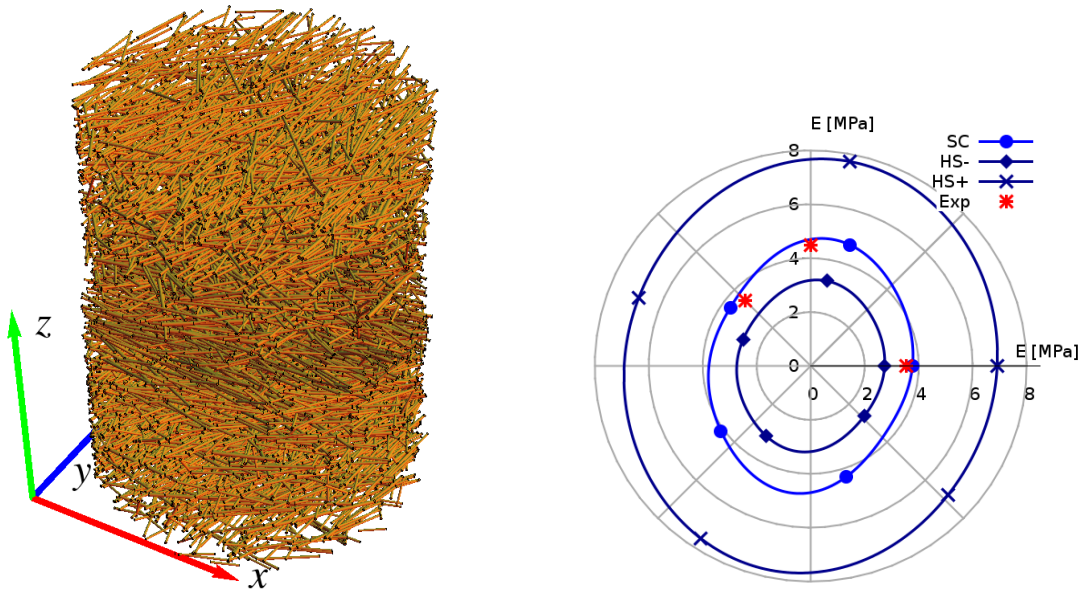

(a) (b)

Figure 1. (a) Reconstruction of the segmented μCT data; (b) Isospherical projection of the direction-dependent Young's modulus in comparison with experimental results.

where $\boldsymbol{d}$ is the direction vector parametrized in spherical coordinates. In Fig. 1(b), the homogenization results are compared with experimental measurements. In this figure, the isospherical projection of the shape of the direction-dependent Young's modulus on the plane, from which the tensile specimen have been prepared, is shown. It can be seen, that the experimental and the SC results are located between the two-step results. The admissible range for the elastic properties bounded by the two-step methods amounts to about 5MPa. Compared with the experimental measurements, the SC method predicts higher Young's modulus in all directions. The difference ranges between 0.23 and 0.31MPa.

1.6. Conclusions

The discussed mean field homogenization approaches are capable of handling the segmented μCT data and taking into account the anisotropic distribution of the fiber axes, the length, and the radius distribution. Operating on this discretized data, the considered methods deliver anisotropic elastic stiffnesses. The anisotropy is caused by the microstructure properties. In the discussed cases, the self-consistence homogenization method based on the segmented μCT data predicts a stiffer material behavior compared to tensile test.

2. Estimation of the fiber orientation distribution function

2.1. Introduction

The distribution of the fiber orientations is an essential attribute of the microstructure of SFRCs. Especially in shell-like injection molded parts, it has been frequently observed, that the fibers

are oriented in layers [1]: In the boundary layers, the fibers are predominantly oriented in the filling direction and in the core layer perpendicular to it. The one point statistics of the fiber orientations can be described with fiber orientation distribution functions (FODF) or with an infinite set of fiber orientation tensors. In mold flow simulations, usually, the mean fiber orientation distribution is described by second order fiber orientation tensors. These tensors are used in conjunction with closure approximations to estimate the fourth order fiber orientation tensors. The orientation tensor of fourth order is then utilized to estimate the effective properties of the composite.

In this work, it is shown, how the FODF can be approximated, if only discrete fiber orientations or the leading fiber orientation tensors are available. Since these tensors can not describe the orientation distribution entirely, a unique solution for this so-called moment problem does not exist.

2.2. Properties of the fiber orientation distribution function

The orientation of a fiber axis can be described with a unit vector $\boldsymbol{n}$. The FODF specifies the volume fraction of all fibers with a certain orientation $\boldsymbol{n}$ (see, e.g. [2]):

$$\frac{\mathrm{d}v}{v}(\boldsymbol{n}) = f(\boldsymbol{n})\,\mathrm{d}S, \tag{8}$$

where $\mathrm{d}S$ is a surface element of the unit sphere $S := \{\boldsymbol{n} \in \mathbb{R}^3 : \|\boldsymbol{n}\| = 1\}$. In general, a density function like the FODF is normalized and always non-negative:

$$\int_S f(\boldsymbol{n})\,\mathrm{d}n = 1, \qquad f(\boldsymbol{n}) \geq 0\ \forall \boldsymbol{n} \in S. \tag{9}$$

A fiber does not have an explicit direction. Thus, the orientations indicated by $\boldsymbol{n}$ or $-\boldsymbol{n}$ are equal:

$$f(\boldsymbol{n}) = f(-\boldsymbol{n}). \tag{10}$$

2.3. Empirical fiber orientation distribution function

For N equal weighted fiber orientations $\boldsymbol{n}$, the empirical FODF $f(\boldsymbol{n})$ is defined as

$$f(\boldsymbol{n}) = \frac{1}{N}\sum_{\alpha=1}^{N} \delta(\boldsymbol{n} - \boldsymbol{n}_\alpha). \tag{11}$$

Herein, $\delta(\boldsymbol{n} - \boldsymbol{n}_\alpha)$ is the Dirac delta distribution on unit vectors.

2.4. Fiber orientation tensors

Kanatani [6] distinguished three different kinds of fiber orientation tensors. The *fiber orientation tenors of the first kind* are averages of the dyadic products of the directions $\boldsymbol{n}_\alpha$:

$$\int_{S^2} f(\boldsymbol{n})\,\boldsymbol{n}^{\otimes\beta}\,\mathrm{d}n = \frac{1}{N}\sum_{\alpha=1}^{N} \boldsymbol{n}_\alpha^{\otimes\beta} = \boldsymbol{N}_{\langle\beta\rangle}, \tag{12}$$

whereas, $\boldsymbol{n}_\alpha^{\otimes\beta}$ specifies a $(\beta-1)$-times tensor product. These tensors are symmetric and, since the FODF is an even function, they are of even rank. A contraction of an β-order tensor reduces the rank by two:

$$\boldsymbol{N}_{\langle\beta\rangle}[\boldsymbol{I}] = \boldsymbol{N}_{\langle\beta-2\rangle}\ \forall\beta \in \{2,4,6,\dots\}. \tag{13}$$

Hence, the fiber orientation tensors of the first kind are not linearly independent. Thus, it is sufficient to use only the β-order tensor for the βth approximation of the FODF.

Fiber orientation tensors of the third kind are symmetric and completely traceless. Such tensors are called deviatoric tensors or irreducible tensors. Using these tensors, the polynomial expansion of the FODF becomes

$$f(\boldsymbol{n}) = D + \sum_{\alpha=1}^{\infty} \boldsymbol{D}_{\langle 2\alpha\rangle} \cdot \left(\boldsymbol{n}^{\otimes 2\alpha}\right)'. \tag{14}$$

In the last equation, $\boldsymbol{D}_{\langle s\rangle}$ are irreducible tensors:

$$\boldsymbol{D}_{\langle\alpha\rangle} = \frac{2\alpha+1}{2^\alpha}\binom{2\alpha}{\alpha}(\boldsymbol{N}_{\langle\alpha\rangle})'. \tag{15}$$

All $\boldsymbol{D}_{\langle\alpha\rangle}$ are orthogonal to each other in terms of the inner product

$$(f,g) = \int_{S^2} f\,g\,\mathrm{d}n = 0. \tag{16}$$

In order to fulfill the normalization condition in equation (9), D is usually chosen equal to one.

2.5. Maximum entropy method

The inherent incompleteness of measured data implies ill-posed mathematical problems, which do not have unique solutions. With the *maximum entropy method* (MEM) it is possible to single out one solution by choosing the solution with the maximum entropy. Shannon [10] identified a quantity in the context of information theory, that is a measure of uncertainty of an information source. Due to the related meaning and the equivalent mathematical formulation of this quantity to the entropy in thermodynamics, it is called *Shannon's-entropy* or *information-theoretic entropy*. Jaynes [4, 5] introduced the MEM in the area of statistical mechanics. A comprehensive overview of the MEM is given in [12].

The information-theoretic entropy is defined by

$$\mathcal{S} = -\int_S f(\boldsymbol{n}) \ln\left(f(\boldsymbol{n})\right) \mathrm{d}S \quad \in (-\infty, 0], \tag{17}$$

where $f(\boldsymbol{n})$ is an orientation distribution function. For an uniform distribution the information-theoretic entropy is equal to zero.

Moment Problem Since the moment of the function $\boldsymbol{n}^{\otimes\alpha}$ regarding the density function $f(\boldsymbol{n})$ is computed by

$$\langle \boldsymbol{n}^{\otimes\alpha}\rangle = \boldsymbol{N}_{\langle\alpha\rangle} = \int_S f(\boldsymbol{n})\,\boldsymbol{n}^{\otimes\alpha}\,\mathrm{d}S \tag{18}$$

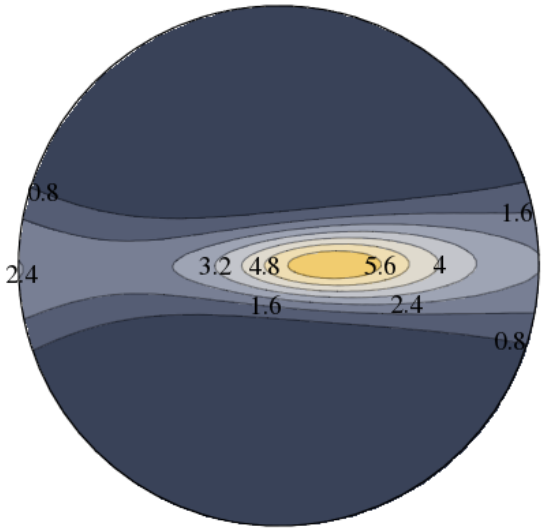

Figure 2.

$\forall \alpha = \{2, 4, \dots\}$, fiber orientation tensors $\boldsymbol{N}_{\langle\alpha\rangle}$ can be considered as averages or expectations of the corresponding functions $\boldsymbol{n}^{\otimes\alpha}$. Thus, the operation denoted by $\langle\cdot\rangle$ depicts an orientation averaging process.

In order to approximate the density function $f(\boldsymbol{n})$ by a function $\bar{f}(\boldsymbol{n})$ using N given moment tensors $\{\boldsymbol{D}_{\langle 2\rangle}, \dots, \boldsymbol{D}_{\langle N\rangle}\}$, the moment problem is stated as follows:

$$\begin{aligned} \bar{\mathcal{S}} &= -\int_S \bar{f}(\boldsymbol{n}) \ln\left(\bar{f}(\boldsymbol{n})\right) \mathrm{d}S \quad \rightarrow \quad \max, \\ C_0 &:= \int_S \bar{f}(\boldsymbol{n}) \, \mathrm{d}S - 1 \stackrel{!}{=} 0, \\ \boldsymbol{C}_{\langle\alpha\rangle} &:= \int_S \bar{f}(\boldsymbol{n}) (\boldsymbol{n}^{\otimes\alpha})' \, \mathrm{d}S - \boldsymbol{D}_{\langle\alpha\rangle} \stackrel{!}{=} 0, \end{aligned} \tag{19}$$

where α is even and ranges from 2 to N. In this nonlinear constrained maximization problem, fiber orientation tensors of the third kind are used. The first side condition C_0 respects the normalization condition in equation (9.1). The normalization of a density function is equal to chose $D = 1$ in the expansion of the FODF in equation (14). The additional side conditions demand, that the appropriate given moment tensor is reproduced by the estimation function $\bar{f}(\boldsymbol{n})$. Using the Lagrange multiplier method, this problem can be solved with the following objective functional:

$$\mathcal{F} = \bar{\mathcal{S}} - G_0 C_0 - \sum_{\alpha=1}^{N/2} \boldsymbol{G}_{\langle 2\alpha\rangle} \cdot \boldsymbol{C}_{\langle 2\alpha\rangle}. \tag{20}$$

2.6. Results and Discussion

In Fig. 2, the approximation of the FODF according to the procedure given in the previous section is shown as polefigure. This approximation is based on the second-order fiber orientation tensor of the microstructure shown in Fig. 1(a). The out-of-plane direction in Fig. 2 corresponds to the y-direction in Fig. 1(a). It can be seen, that the main fiber orientation, indicated by the

greatest value in Fig. 2, is not located in y-direction, which is the filling direction during the injection molding process. The anisotropy visible in this figure conforms with the anisotropy of the directional-dependent Young's modulus in Fig. 1(b). Nevertheless, it is also visible, that the fibers with an orientation perpendicular to the filling direction, are not properly considered in this approximation. Therefore, it is reasonable to take into account further orientation information as, e.g., the irreducible tensors of fourth order.

References

[1] A. Bernasconi, F. Cosmi, and P. Hine. Analysis of fibre orientation distribution in short fibre reinforced polymers: A comparison between optical and tomographic methods. *Composites Science and Technology*, 72(16):2002–2008, 2012.

[2] T. Böhlke. Application of the maximum entropy method in texture analysis. *Computational Materials Science*, 32(3–4):276–283, Mar. 2005.

[3] T. Böhlke and C. Brüggemann. Graphical representation of the generalized hooke's law. *Technische Mechanik*, 21(2):145–158, 2001.

[4] E. T. Jaynes. Information theory and statistical mechanics. *Physical Review*, 106(4):620–630, May 1957.

[5] E. T. Jaynes. Information theory and statistical mechanics. II. *Physical Review*, 108(2):171–190, Oct. 1957.

[6] K.-I. Kanatani. Distribution of directional data and fabric tensors. *International Journal of Engineering Science*, 22(2):149–164, 1984.

[7] V. Müller, B. Brylka, T. Böhlke, F. Dillenberger, R. Glöckner, and S. Kolling. Homogenization of elastic properties of short fiber-reinforced composites based on measured microstructure data. 2014 submitted.

[8] P. Ponte Castañeda and P. Suquet. Nonlinear composites. *Advances in Applied Mechanics*, 34:171–302, 1997.

[9] H. Schürmann. *Konstruieren mit Faser-Kunststoff-Verbunden*, volume 2 of *VDI-Buch*. Springer-Verlag, Berlin-Heidelberg, 2007.

[10] C. Shannon. A mathematical theory of communication. *Bell System Technical Journal*, 27(3):379–423, 1948. WOS:A1948UH03900001.

[11] J. R. Willis. Bounds and self-consistent estimates for the overall properties of anisotropic composites. *Journal of the Mechanics and Physics of Solids*, 25(3):185–202, 1977.

[12] N. Wu. *The maximum entropy method*. Number 32 in Springer Series in Information Sciences. Springer, Berlin, 1997.